We would like to thank referee #1 for the valuable and constructive comments. We address all comments (in italic bold) and specify the position of the proposed updated text.

Comment 1

My major concern is that the parameterization has been tuned and validated for the same wind farm (Section 4.1.1). Results herein presented are therefore a maximum limit on the performance of the scheme. Ideally you should calibrate the parameterization on an independent wind farm. If this is not possible you should show results of the sensitivity simulations you performed to select the parameter of the parameterization, σ_0.

The reviewer is right that ideally the initial length scale should be determined from the measurements at an independent wind farm. Unfortunately, we don't access long-term measurements from other wind farms. As stated in the text, we have tried to use the available observations in an as independent manner as possible:
1) we use the turbine data that represents a rotor swept area averaged wind speed to determine the initial length scale σ_0. Then, we use point measurement met mast wind speeds at 2 km and 6 km downstream for the validation. 2) the wind farm data and the met mast data are from two different sub-sets, since they have different filter criteria (turbine measurements have the additional requirement that they are only selected when up-stream turbines are operation). 3) The initial length scale has been determined from one wind speed bin (9 m/s), whereas we validated the scheme for five wind speed bins.

As proposed by the reviewer, we have updated Fig. 4, which now shows the sensitivity of the initial length scale within the wind farm. The plot has been attached at the end of the document (incl. updated caption). Related to the Fig. 4, we propose the following change on p. 3495 l. 20–21:

> Figure 4 shows the results from the simulations with $\sigma_0 = 1.7\,R_0$, which had the smallest overall bias compared to the measurements.

to:

> The lines in Fig. 4 show the results from the simulations with $\sigma_0 = 1.7\,R_0$, which had the smallest overall bias compared to the measurements. Additionally, the coloured dots indicate the sensitivity to the initial length scale for σ_0 =1.5 and $1.9\,R_0$.

Comment 2

Having the scheme tuned for this particular wind farm somewhat hampers the comparison with the WRF-WF parameterization that has not been tuned for this particular wind farm. This should be clarified.

As has been mentioned in the previous comment, the EWP scheme uses the initial length scale, σ_0, that has been tuned by the measurements inside the Horns Rev I wind farm. The WRF-WF scheme on the other hand has no free parameters. Their drag force depends on the turbine specific thrust curve and the additional turbulence on the difference between the thrust and power curve (Eq. 16 on p. 3496 l. 7). Therefore, it was remarkable that the velocity at hub-height was almost identical in the EWP and WRF-WF scheme at the end of the wind farm (although the structure of the velocity profiles differed). The validation was performed in the wake recovery of the wind farm were the schemes are not active anymore.

To clarify that the WRF-WF scheme has no tunable constants, we propose to change on p. 3496 l. 23:

> This approach is used in the experiments performed in Sect. 5.

to:

> In Sect. 5, we use the up-dated WRF-WF parametrisation from WRFV3.6. Its input parameters, the power and thrust curve, come from the Vestas V80 turbine.

Also, we would mention more explicitly in the introduction of section 5 on p. 3497 l. 1–6 that the EWP scheme uses a calibrated initial length scale from the wind farm data and change:

> To obtain a complete picture of the modelled velocity field within and downstream of the Horns Rev I wind farm, we compare the hub-height velocity simulated by the WRF model using the two wind farm parametrisations for one wind speed bin. We used the second most frequently observed wind speed bin (10 m s^1), which is different from that used in the calibration (Sect. 4.1.1), to be as calibration independent as possible. Afterwards, we compare the modelled velocities for all wind speed to the measurements at M6 (2 km downstream) and M7 (6 km downstream).

to:

> To obtain a complete picture of the modelled velocity field within and downstream of the Horns Rev I wind farm, we compare:
> (I) the hub-height velocity simulated by the WRF model using the two wind farm parametrisations for the $10\,\mathrm{m\,s^{-1}}$ wind speed bin. We recall that the initial length scale of the EWP scheme has been determined at $9\,\mathrm{m\,s^{-1}}$.
> (II) the modelled velocities to the measurements at M6 (2 km downstream) and M7 (6 km downstream) for all five wind speeds (7, 8, 9, 10, and $11\,\mathrm{m\,s^{-1}}$).

In the discussion, we propose to add the here underlined text on p. 3503 l. 18–22:

Before we validated the results of the schemes in the wake of the wind farm, the a priori unknown initial length scale of the EWP scheme had to be determined. We did this using the turbine power measurements from the most frequently observed wind speed bin. This limitation could not be avoided, since to our knowledge no other long-term measurements from large offshore wind farms were available. On the other hand, for the WRF-WF scheme we have used the turbine specific thrust and power curves, which are its only input parameters.

Comment 3

Finally, it seems the authors have available a large observational dataset but have restricted the comparison for westerly winds with different atmospheric conditions. If possible, the authors should extend the validation showing more specific results of the parameterizations performance (e.g. wind farm wakes as a function of the hub height wind speed). I do not see a major reason for not including a more extended comparison having the data and the simulations available.

As discussed in section 3, the met masts that have been used in the validation are located to the East of the Horns Rev I wind farm. Therefore, wind farm wakes can only be captured at the met masts when the wind blows from the west.
For this wind direction sector, we used all wind speeds between 7 m/s (to be above the cut-in wind speed of 4 m/s in the entire wind farm) and 11 m/s (to be below the wind speed were pitch control starts, 13 m/s). In Fig. 5, we show the downstream velocity recovery for the 10 m/s wind speed bin. Then, Fig. 6 compares for all selected wind speed bins (7, 8, 9, 10, and 11 m/s), the modelled wind speed at the met masts to that of the measurements. Therefore, figures similar to Fig. 5 for additional wind speeds would not provide any additional information, since Fig. 6 shows the recovery for all wind speed bins.

SPECIFIC COMMENTS

1. Page 3485, Line 12: it will be good if you can describe the ensemble-average methodology, its differences with the more standard approach of volume averaged shown in Fig. 1, and why is relevant for the EWP wind farm parameterization.

The description of the averaging is an important part of the paper, we propose therefore to update section 2.2 and Fig. 1. To support the description of the averaging procedure in more detail we have prepared an additional Appendix (attached).

1) In the new Appendix, we would adapt the notation of Raupach and Shaw (1982) for the double averaging. For consistency, we would change to this notation in the whole paper. Therefore, we propose to substitute on p. 3485 l. 11–12:

> We will use the notation and symbols of Wyngaard (2010). The upper-case letters refer to ensemble-averaged quantities, whereas lower-case letters refer to fluctuations.

with:

> We use an over-line to denote ensemble-averaged quantities and a prime for a fluctuation around the ensemble average.

2) Regarding the averaging, we have edited Fig. 1 (attached below) and we propose to substitute on p. 3486 l. 12–21:

> The previously defined variables in the Eqs. (1) and (3) have to be redefined on the three-dimensional model grid. A new volume-averaged velocity equation is derived by integrating Eq. (1) over the grid-cell volume. For Eq. (3), we define a (random) velocity fluctuation at any hypothetical measurement point within a grid-cell volume to be the difference between the ensemble-averaged and the instantaneous velocity. This is illustrated schematically in Fig. 1a. Then, the grid-cell averaged TKE can be thought of as the variance of the velocity fluctuations around the ensemble-averaged velocity and not around the grid-cell averaged velocity as shown in Fig. 1b.
> The aim is to obtain expressions for the terms P_t (Eq. 3) and F_D (Eq. 1) that are consistent with the mesoscale model flow equations. The expression for Pt can be found by multiplying the NavierStokes equations with the velocity fluctuation and then applying Reynolds averaging. This gives for the additional source term:
>
> $$P_\mathrm{t} = \overline{\rho\, A_\mathrm{r}\, c_\mathrm{T}\, (U_i + u_i)^2\, u_i}/2 \sim \rho\, A_\mathrm{r}\, C_\mathrm{T} U \overline{u_i^2}, \tag{4}$$
>
> where $\rho\, A_\mathrm{r}\, c_\mathrm{T}\, (U_i + u_i)^2$ is the instantaneous forcing due to the action of the wind turbine, the lower case c_T the instantaneous thrust coefficient, the upper case C_T the averaged thrust coefficient, and Ar the rotor area.

with:

The previously defined variables in the Eqs. (1) and (3) have to be redefined on the three-dimensional model grid. We use angle brackets to denote the volume average. The aim is to obtain expressions for the terms $\langle\, \overline{f_d}\,\rangle$ and $\langle\, \overline{p_t}\,\rangle$ for the wind farm parametrisation that are consistent with the mesoscale model flow equations.

A new volume-averaged velocity equation is derived by integrating Eq. (1) over the grid-cell volume. This gives the expression for $\langle\, \overline{f_d}\,\rangle$, which is derived in the following section 2.2.1.

The derivation of the source term $\langle\, \overline{p_t}\,\rangle$ depends on the definition of the velocity perturbation. Formally, a velocity perturbation is the difference between the instantaneous and ensemble-averaged velocity. For homogeneous flows, the spatial-averaged velocity can be used for the definition of a velocity fluctuation, since the ensemble average can be approximated by the spatial average. However, the flow around wind turbines is non-homogeneous and consequently the spatial and ensemble average deviate. This has been illustrated in Fig. 1. Double averaging (ensemble and spatial) allows to separate the total kinetic energy into three contributions. Then, the source term $\langle\, \overline{p_t}\,\rangle$ in the TKE equation depends on the definition of mean and turbulence kinetic energy. In Appendix A, we discuss in more detail the double averaging and the ways mean and turbulence kinetic energy can be described.
In the EWP scheme, we follow Raupach and Shaw (1982) and Finnigan and Shaw (2008) and define a turbulence fluctuation around the ensemble mean (Approach I in Appendix A). With this definition, we include only the random motion in the TKE. The expression for the volume-averaged $\langle\, \overline{p_t}\,\rangle$ can then be found by multiplying the Navier-Stokes equations with the velocity fluctuation and then applying Reynolds averaging. This gives for the source term:

$$\langle\, \overline{p_t}\,\rangle = \langle\, \overline{u_i'\, f_i'}\,\rangle \approx -\frac{1}{2}\,\rho\, A_r\, c_\mathrm{t} \langle\, \overline{u_{i,h}^2\, u_{i,h}'}\,\rangle \approx -\,\rho\, A_\mathrm{r}\, c_\mathrm{t}\, \langle\, \overline{u_{i,h}}\, \overline{u_{i,h}'^2}\,\rangle, \tag{4}$$

where $\rho\, A_r\, c_\mathrm{t}\, u_{i,h}^2/2$ is the instantaneous forcing due to the action of the wind turbine, c_t the thrust coefficient, A_r the rotor area, and h the turbine hub-height.

3) Because of the changed Fig. (1) and the additional Appendix A, we propose furthermore to up-date on p. 3496 l. 12–14 in Sect. 4.1.2:

The same result, $P_{t,\mathrm{WRF\text{-}WF}} = \rho\, A_\mathrm{r}\, C_\mathrm{T}\, a\, \overline{u}^3/2$, can also be obtained by defining a velocity fluctuation as the difference between the grid-cell averaged velocity and the instantaneous velocity as illustrated in Fig. 1b.

to:

The same result, $\langle \overline{p_t}_{,\text{WRF-WF}} \rangle = \rho A_\text{r} c_\text{t} a \langle \overline{u} \rangle^3/2$, is also obtained by defining a velocity fluctuation as the difference between the grid-cell averaged velocity and the instantaneous velocity (Approach II in Appendix A). In Fig. 1, we illustrated a wake and the difference between the grid-cell averaged velocity (red line) and the instantaneous velocity (grey line) is denoted by u''.

2. Page 3487, lines 5-10: If I understood correctly, the turbulence induced by the rotor is dissipated within the grid cell and Pt is neglected on Eq. 3. This probably has implications for the maximum horizontal resolution that can be achieved by the parameterization. Is there any theoretical/empirical limit?

As the second referee pointed out in his fourth comment, Eq. (4) should have a minus sign. This term would therefore be a sink of TKE. This has no implications on the results, since we have neglected the additional term in Eq. (4).

3. It is not clear to me what are the final equations that are implemented on the WRF model. I think the parameterization only needs to incorporate equations 14 and 15 in the model. Is this correct?

The reviewer is correct that Eqs. (14) and (15) apply the turbine induced drag force to the model's RANS equation. Additionally, Eq. (12) is implemented to determine the effective length scale of the vertical wake extension.

We propose to replace on p. 3491 l. 2–3:

> For each turbine a thrust force is calculated with Eqs. (14) and (15). The total thrust force for a turbine containing grid-cell is then obtained from a superposition of the single turbine thrust forces and is added to the numerical approximation of Eq. (1).

with:

> In the numerical model, Eqs. (14) and (15) are added to the numerical approximation of Eq. (1). Furthermore, Eq. (12) is used to determine the effective length scale σ_e of the vertical wake extension. At every time-step the total thrust force within a grid-cell is obtained from a superposition of the single turbine thrust forces.

as well as on p. 3491 l. 12–13:

> A practical description of how to use the EWP scheme in the WRF model is given in Sect.

with:

A practical description of how to use the EWP scheme in the WRF model is given in the section "Code availability" at the end of the paper.

4. page 3491, line 11: WRF does not have 2nd order PBL closures.

In the revised manuscript we would substitute on p. 3491 l. 11:

second order → 1.5 order

5. Page 3493, line 14, is there any specific reason to select the horizontal resolution of 1120m? Why not just 1 km?

This value was chosen to accommodate the uniform spacing of the turbines in the Horns Rev I wind farm. The turbine spacing is 560 m in the West-East direction. Consequently, with a 1120 m horizontal grid-spacing, we obtain in the flow direction a constant number of turbines per grid-cell within in wind farm. In the cross-stream direction, we have defined only one turbine row in the most northern and southern grid-cell, since these rows were not included in the row averaging in the measurements (p. 3495 l. 10–11).

We propose to add the here underlined sentence to p. 3493 l. 14:

... Δ x = Δ y = 1120 m. <u>This horizontal grid-spacing, which is twice the turbine separation, guarantees a constant number of turbines per grid-cell in the flow direction.</u> Equally to the Horns rev I wind farm ...

6. Page 3494, line 11, It is not clear how do you impose the wind speed at the hub height. You mention that you integrate the model for four days and use the resulting wind profile to initialize the wind farm simulations. How do you get the hub height winds that you want to impose?

In the idealised case studies the model is initialised with a constant geostrophic wind. During the simulation period a logarithmic profile develops within the boundary layer. To be certain that the wind speeds converge to a given value, we performed a 4 day simulation for every wind speed and wind direction. For every simulation, we impose a geostrophic wind such that after the entire simulation period of 4 days the hub-height wind speed and the wind direction correspond to the measurement binned values. We found the right geostrophic wind by conducting several experiments. The atmospheric state of that instance is used as a restart file for the wind farm and the background simulation without wind farm, such that all necessary variables for the initialisation of the model are saved. Although the atmospheric state converged after 4 days, we still performed the background

simulation to account for the small oscillations around the steady state ($\pm 0.02\,\mathrm{m/s}$).

In the revised manuscript, we propose to add the here underlined sentence on p. 3494 l. 11:

> ... The atmospheric state of each of these 135 simulations was used to drive: a control simulation without wind farm parametrisation, a simulation with the WRF-WF scheme, and a simulation with the EWP scheme. We used the restart option in the WRF model to initialise these simulations. Each control or wind farm simulation lasts one day, resulting in a total simulation length of five days. The wind speeds in the control simulations were 7, 8, 9, 10, and 11 $\mathrm{m\,s^{-1}}$ at 70 m (hub-height) after 5 days of simulation. We found the right geostrophic wind by conducting several experiments. ...

7. How do you represent the turbulent fluxes at the surface (i.e. sensible heat, latent heat and momentum?) in the idealized experiments?

The atmosphere in the idealised case simulations is dry (p. 3494 l. 4). The surface heat flux was set to zero (p. 3493 l.19). Therefore, the slightly stable initial atmosphere converged to a completely neutral atmosphere (p. 3494 l. 6). The momentum flux is determined by the mynn_surface layer scheme. We defined a constant roughness length of 0.0002 m for the whole domain and all points represent water (p. 3493 l. 20–21). Consequently, the friction velocity is determined by the mynn_surface layer scheme from the Charnock formula. All the initial profiles and namelist options are included in the link to the available code at the end of the article.

We propose to change on p. 3493 l. 20:

> The surface roughness was constant in time and set to $z_0 = 2 \times 10^{-4}\,\mathrm{m}$ for the entire domain.

to:

> The domain is fully contained over water and it had a constant roughness length of $z_0 = 2 \times 10^{-4}\,\mathrm{m}$ in time, which follows the WMO standards. The friction velocity is obtained with the Charnock formula.

and add to Table 2:

Surface layer scheme:	MYNN Monin-Obukhov similarity theory (option 5)
TKE advection:	Yes
Roughness length (m):	2×10^{-4}

8. Page 3494, line 17. Are the simulated wind speeds stable enough to use only the instantaneous wind speed in the validation? Usually you average results over a certain temporal period.

All simulations have reached a steady state and therefore it is not necessary to average over time. The amplitude of the oscillations in wind speed at hub-height was less than 0.02 m/s for the final day.

In the revised manuscript we would explicitly mention that we use the converged wind speed and propose to add the here underlined part of the sentence to p. 3497 l. 12–13:

> In the validation, we use the instantaneous model outputs from the converged flow field after the 5 days integration period.

9. Page 3495, lines 23-24: Does sigma0 depend on the horizontal resolution?

This is an interesting question. The initial length scale, σ_0, is not expected to depend on the horizontal grid-spacing. However, this can not be tested easily, since the effective length scale σ_e in Eq. (12) depends on the the horizontal grid-spacing.

10. Page 3495, lines 24-36: I do not understand how you reached this conclusion "Therefore, we conclude that for neutral conditions the initial length scale can assumed to be independent of the upstream conditions." Please, clarify.

Thank you for this comment. We intended to state that the value of $\sigma_0 = 1.7\,R_0$ should apply to similar types of turbines. Therefore, it was not appropriate to use "conclude". We propose to delete this sentence on p. 3495 l. 24–26 and to add to on p. 3503 l. 22 the here underlined sentence:

> ... farms are available. We found for the most frequently observed wind speed bin an initial length scale of $\sigma_0 = 1.7\,R_0$ that fitted the turbine measurements the best. We recommend this constant for similar wind turbines. Future wind turbine measurements are needed to confirm this value for other turbine types, such as low induction turbines. This constant ...

11. Page 3497, lines 4-6: You mentioned before that you used different wind speeds at the hub height for validation but here you say that you use 10 m/s. This deserves clarification.

The simulations with a 10 m/s wind speed were used for the visual analysis related to Fig. 5 (wake recovery compared to measurements), Fig. 7 (analysis of the horizontal wake extension and orientation), and Fig. 8 (qualitative comparison for cross-section of TKE). Additionally, we validate the velocity recovery for all wind speeds (7, 8, 9, 10, and 11 m/s)

in Fig. 6.

This comment is addressed in the introduction of Sect. 5, see response to the second major comment.

12. Same lines as before. Although you use different wind speeds to select sigma0 and validate the parameterization, you focus on the same wind farm and therefore the parameterization is somewhat tuned for this particular site. This hampers the comparison with the WRF-WF parameterization. If you show sensitivities to the values of sigma0 one can have an idea of how important is the specification of this parameter for the results. See also general comment.

This comment is very related to the first major comment, where we have addressed this issue.

13. Would you recommend using the sigma0 herein presented for other wind farms? Or should sigma0 be adjusted for each wind farm?

The initial length scale should be valid for any wind farm. In the future, as more data becomes available, we should be able to verify this hypothesis for different turbine types, such as low induction turbines (with a lower thrust coefficient). See also the answer to comment 10.

14. Page 3499, lines 6-7: The bias in the WRF-WF is not statistically significant. Both the WRF-WF and EWP reproduce the observations within the observational uncertainty.

The reviewer is right that both schemes are within the observational uncertainty, see Fig. 5. On p.3499, l. 6–7, we discuss the bias between the average of the measured wind speed and the modelled wind speed at the 2 met masts, as well as its tendency for different wind speeds.

In the discussion of Fig. 5, we propose to change on p. 3498 l. 4–10:

However, the velocity 2 km downstream of the wind farm, at M6, differs between the schemes by 4.7%. This is important, especially if it was used to estimate the power production on a neighbouring wind farm that was located at this distance from the original wind farm. For example, the Rødsand 2 and Nysted offshore wind farm in Southern Denmark are separated by a comparable distance.

to:

At M6, 2 km downstream of the wind farm, the modelled velocity for both schemes is within the uncertainty of the measurements, but it differs between the schemes by 4.7%. The near wake recovery is important, especially if it was used to estimate the power production on a neighbouring wind farm that was located at this distance from the original wind farm. For example, the Rødsand 2 and Nysted offshore wind farm in Southern Denmark are separated by a comparable distance.

Furthermore, we propose to change on p. 3499 l. 1–7:

The WRF-WF scheme shows a positive bias in velocity of up-to $0.5\,\mathrm{m\,s^{-1}}$ at M6. This positive bias, between the WRF-WF scheme and the measurements, becomes larger with increasing wind speed. The bias at M6 is a consequence of the too fast modelled wake recovery from the end of the wind farm to M6. Between M6 and the point at which the free-stream velocity is reached again, the modelled wake recovery is slower than that measured. This overall positive bias implies that the modelled velocity with the WRF-WF scheme is overestimated throughout the whole wake. This overall positive bias implies that the modelled velocity with the WRF-WF scheme is overestimated throughout the whole wake.

to:

The WRF-WF scheme shows a positive difference in velocity of up-to $0.5\,\mathrm{m\,s^{-1}}$ at M6. This difference, between the WRF-WF scheme and the measurements, becomes larger with increasing wind speed. The higher modelled velocity at M6 is a consequence of the more rapid recovery of the modelled wake from the end of the wind farm to M6 compared to that of the measurements. Between M6 and the point at which the free-stream velocity is reached again, the modelled wake recovery is slower than that measured. This overall positive difference suggests that the modelled velocity with the WRF-WF scheme is overestimated throughout the whole wake.

15. Pages 3500 and 3502, Section 5.2. I like this section. It shows large differences between the TKE from the two schemes. This is probably the largest difference between the 2 schemes. If possible, the authors should show figures from the other works mentioned during the discussion to facilitate the comparison of results from both TKE fields.

Thank you for this positive comment and the suggestion to add additional figures. Figure 5

from Wu and Porté-Agel (2013) would perhaps be a useful figure to show. We plan to ask their publisher for permission.

16. Section 5.2: Are you advecting the TKE in the WRF-WF runs? I think by default is turned off in WRF but is better to activate it. Activating the TKE advection may change the shape of the TKE field shown on Fig. 8b.

In WRFV3.3 and WRFV3.4 the TKE was advected per default and we used V3.4 for our simulations. The switch for TKE (bl_mynn_tkeadvect) advection with the MYNN scheme has been introduced only in WRFV3.5. Regarding the TKE advection, we addressed this in the updated Table 2, see comments nr. 7.

17. Conclusions, page 3501, lines 25-26. The bias is not statistically significant. Maybe is better to say that EWP reproduces the wind farm wake within the observational uncertainty.

We agree with the reviewer and propose to change on p. 3504 l. 25–26:

> The bias was less than 0.15 $\mathrm{m\,s^{-1}}$, except for the 7 $\mathrm{m\,s^{-1}}$ wind speed bin at mast M6, where it was around 0.23 $\mathrm{m\,s^{-1}}$.

to:

> The EWP scheme reproduces the wind farm wake within the observational uncertainty.

18. Page 3506, line 13: Why do you need the power coefficient? It is not mentioned in the description of the EWP parameterization.

The power is not needed for the wind farm wake simulations. It is used, however, to estimate the power production of the wind turbines.

We propose to add on p. 3506 l.13:

> . . . in a file. Where the power coefficient is used optionally to estimate the turbine power production. This file name . . .

Appendix A

We use the notation and symbols of Raupach and Shaw (1982), with the exception that the ensemble average is used instead of the time average. The instantaneous velocity, u_i, can be decomposed in a spatial average and a fluctuation around it, $u_i = \langle u_i \rangle + u_i''$ and an ensemble average with a fluctuation, $u_i = \overline{u}_i + u_i'$. Figure 1 illustrates the instantaneous velocity, as well as the spatial and ensemble-averaged velocity in the vicinity of a wake.

We can decompose the total kinetic energy:

$$\frac{1}{2}\langle \overline{u_i^2} \rangle = \frac{1}{2}\langle \overline{u}_i^2 \rangle + \frac{1}{2}\langle \overline{u_i'^2} \rangle \tag{5}$$

$$= \frac{1}{2}\langle \overline{u}_i \rangle^2 + \frac{1}{2}\langle \overline{u}_i''^2 \rangle + \frac{1}{2}\langle \overline{u_i'^2} \rangle. \tag{6}$$

In Eq. (5), we applied an ensemble and spatial averaging to the kinetic energy and we have decomposed the ensemble-averaged kinetic energy in an average and fluctuating part. Here, $\frac{1}{2}\langle \overline{u}_i{}^2 \rangle$ is the spatial average of the ensemble-averaged kinetic energy and $\frac{1}{2}\langle \overline{u_i'^2} \rangle$ the spatial average of the kinetic energy from random velocity fluctuations.

By decomposing the first term on the r.h.s. of Eq. (5), we obtain Eq. (6). In Eq. (6), we now have three contributions to the total spatial and ensemble-averaged kinetic energy. The first term $\frac{1}{2}\langle \overline{u}_i \rangle^2$ is the kinetic energy of the spatial and ensemble-averaged velocity. The second term $\frac{1}{2}\langle \overline{u}_i''^2 \rangle$ is the spatial-averaged kinetic energy of the heterogeneous part of the mean flow, which is the difference between the ensemble and spatial-averaged kinetic energy. This term arises only in non-homogeneous flow conditions and is also called "dispersive kinetic energy" by Raupach and Shaw (1982).

For each contribution on the r.h.s. of Eq. (6) to the total kinetic energy, a budget equation can be derived. The complete set of equations can for example be found in Raupach and Shaw (1982). We can combine the three components in Eq. (6) to kinetic energy of the mean flow (MKE) and turbulence kinetic energy (TKE). The MKE is not directly resolved by the model. However, the definition of TKE determines how the effect of wind turbines to the TKE is parametrised.

In approach I, one can define MKE $= \frac{1}{2}\langle \overline{u}_i^2 \rangle = \frac{1}{2}\langle \overline{u}_i \rangle^2 + \frac{1}{2}\langle \overline{u}_i''^2 \rangle$ and TKE $= \langle \frac{1}{2}\overline{u_i'^2} \rangle$ (Raupach and Shaw, 1982; Finnigan and Shaw, 2008). Here, the MKE is equal to the spatial average of the ensemble-averaged kinetic energy and it contains all kinetic energy of the organised motion. With this definition only random motion contributes to the TKE. The presence of the drag force gives rise to the source term $\langle \overline{p}_t \rangle = \langle \overline{u' f'} \rangle$, where f' is the fluctuation of the drag force around the ensemble-averaged force. This approach is used in

the EWP scheme and in Sect. 2.2 the additional source term is derived.

In approach II, one could define MKE $= \frac{1}{2}\langle\, \overline{u}_i \,\rangle^2$ and then the TKE $= \frac{1}{2}\langle\, \overline{u}_i''^2 \,\rangle + \frac{1}{2}\langle\, \overline{u_i'^2} \,\rangle$. In this case, the MKE contains only kinetic energy from the spatial-averaged velocity. Whereas, the TKE contains now also energy from the heterogeneous part of the mean flow additional to the energy from random motion. In this approach, a fluctuation can be decomposed in $u'' = \overline{u}_i'' + u_i'$. Therefore, the source term becomes $\langle\, \overline{p}_t \,\rangle = \langle\, \overline{u'' f''} \,\rangle$, where f'' is the fluctuation of the drag force around the spatial averaged-force. In the WRF-WF, this approach is used (see Sect. 4.1.2).

References

Finnigan, J. J. and Shaw, R. H.: Double-averaging methodology and its application to turbulent flow in and above vegetation canopies, Acta Geophysica, 56, 534-561, doi:10.2478/s11600-008-0034-x, 2008.

Nakanishi, M. and Niino, H.: Development of an improved turbulence closure model for the atmospheric boundary layer, J. Meteorol. Soc. Jpn., 87, 895–912, 2009.

Raupach, M. R. and Shaw, R. H.: Averaging procedures for flow within vegetation canopies, Bound.-Lay. Meteorol., 22, 79–90, doi:10.1007/BF00128057, 1982.

Wu, Y.-T. and Porté-Agel, F.: Simulation of turbulent flow inside and above wind farms: model validation and layout effects, Bound.-Lay. Meteorol., 146, 181–205, 2013.

Wyngaard, J. C.: Turbulence in the Atmosphere, Cambridge Press, Cambridge, UK, 2010.

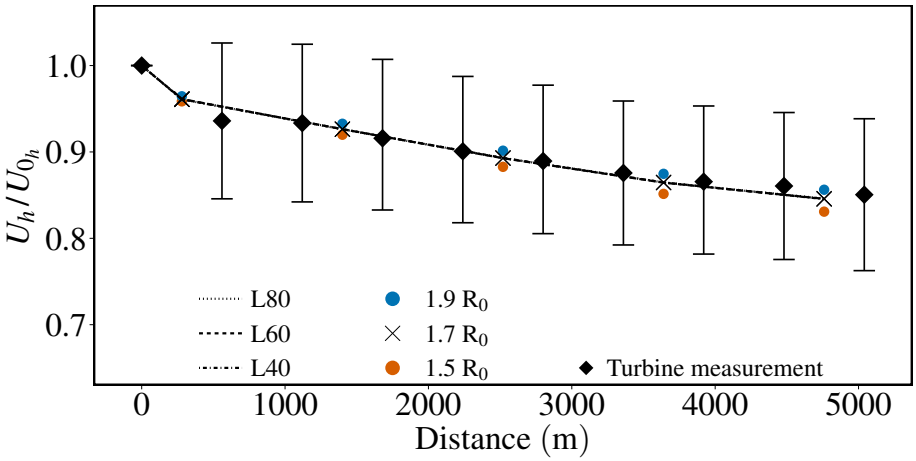

Figure 4: Measured and simulated hub-height velocity within the wind farm. The lines show the model simulated velocities averaged over wind direction with an initial length scale $\sigma_0 = 1.7\,R_0$ for the 3 vertical resolutions (L40, L60, and L80). The diamonds represent the measured turbine velocity averaged over each row and the bars indicate their standard deviations. The crosses mark the velocity at the grid-cell centre. The normalised velocity for $\sigma_0 = 1.5\,R_0$ and $\sigma_0 = 1.9\,R_0$ is shown with red and blue dots.

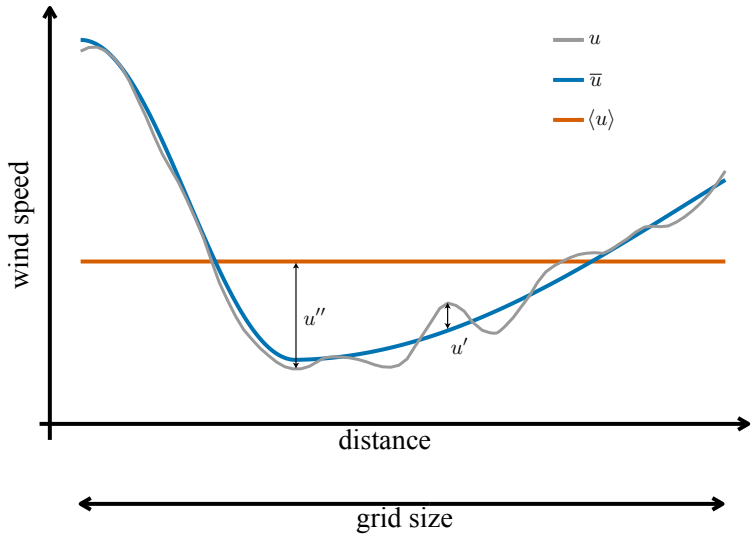

Figure 1: A sketch of the downstream development of a turbine induced velocity reduction. The x-axis indicates the grid-cell size. The grey line represents the instantaneous velocity and the coloured lines the averaged values. The difference between the average and instantaneous velocity defines the turbulence fluctuation at each distance.